

The in vitro immunomodulatory effect of multi-walled carbon nanotubes by multilayer analysis

Veera Hautanen^{a,c}, Jack Morikka^a, Laura Aliisa Saarimäki^a, Jan Bisenberger^a, Tarja Toimela^a, Angela Serra^{a,b}, Dario Greco^{a,c,d,*}

^a Finnish Hub for Development and Validation of Integrated Approaches (FHAIVE), Faculty of Medicine and Health Technology, Tampere University, Arvo Ylpön katu 34, Tampere 33520, Finland

^b Tampere Institute for Advanced Study, Tampere University, Kalevantie 4, Tampere 33100, Finland

^c Institute of Biotechnology, University of Helsinki, P.O.Box 56, Helsinki, Uusimaa 00014, Finland

^d Division of Pharmaceutical Biosciences, Faculty of Pharmacy, University of Helsinki, Finland

ARTICLE INFO

Editor: Dr. Phil Demokritou

Keywords:

Multi-walled carbon nanotube

Immunotoxicity

THP-1

Macrophage

In vitro model

ABSTRACT

The study of multi-walled carbon nanotube (MWCNT) induced immunotoxicity is crucial for determining hazards posed to human health. MWCNT exposure most commonly occurs via the airways, where macrophages are first line responders. Here we exploit an in vitro assay, measuring dose-dependent secretion of a wide panel of cytokines, as a measure of immunotoxicity following the non-lethal, multi-dose exposure (IC5, IC10 and IC20) to 7 MWCNTs with different intrinsic properties. We find that a tangled structure, and small aspect ratio are key properties predicting MWCNT induced immunotoxicity, mediated predominantly by IL1B cytokine secretion. To assess the mechanism of action giving rise to MWCNT immunotoxicity, transcriptomics analysis was linked to cytokine secretion in a multilayer model established through correlation analysis across exposure concentrations. This reinforced the finding that tangled MWCNTs have greater immunomodulatory potency, displaying enrichment of immune system, signal transduction and pattern recognition associated pathways. Together our results further elucidate how structure, length and aspect ratio, critical intrinsic properties of MWCNTs, are tied to immunotoxicity.

1. Introduction

The versatile applications of multi-walled carbon nanotubes (MWCNT), has led to a significant increase in their production and use (De Volder et al., 2013; Beg et al., 2011; Cheng et al., 2021; Dong et al., 2015a; Klumpp et al., 2006). At the same time as their increased use, the toxicity of MWCNTs is being recognized, with endpoints such as pulmonary toxicity, genotoxicity, carcinogenicity and immunotoxicity (Kobayashi et al., 2017; Fukushima et al., 2018; Fraser et al., 2020). One of the principal means of toxic exposure to MWCNTs is through inhalation, resulting in pathologies of the pulmonary system (Dong et al., 2015b; Umeda et al., 2013). Biopersistence of carbon nanomaterials in the lung can be chronic with aerosolized and inhaled MWCNTs (Mercer et al., 2013). Repeated inhalation of MWCNTs, coupled with biopersistence, leads to epithelial injury and altered immune regulation (Rydman et al., 2014; Poulsen et al., 2016; Kinaret et al., 2017). Rodent

studies have linked CNT exposure to pulmonary fibrosis and pulmonary carcinogenesis (Dong et al., 2015b; Nagai et al., 2011; Sargent et al., 2014; Chen et al., 2014), prompting organizations such as the CDC and NIOSH to issue guidelines on exposure, citing inhalation of aerosolized CNTs during manufacture as the primary exposure risk, with dermal contact and ingestion also considered (Oberdörster et al., 2015; CDC, 2013). Due to this toxic potential, the study of MWCNT exposure is becoming increasingly important, and mechanistic analyses that deconstruct biological responses to the increasingly large array of commercial MWCNTs are necessary. The varied structural properties of MWCNTs can change the biological response to their exposure, and attempts have been made to measure how differences in these structural properties confer intracellular effects and, subsequently, extracellular consequences (David et al., 2016). The three dimensional structural properties of length, diameter, aspect ratio, surface area and the overall shape of the material, alter how cells recognize and interpret MWCNTs

* Corresponding author at: Finnish Hub for Development and Validation of Integrated Approaches (FHAIVE), Faculty of Medicine and Health Technology, Tampere University, Arvo Ylpön katu 34, Tampere 33520, Finland.

E-mail address: dario.greco@tuni.fi (D. Greco).

<https://doi.org/10.1016/j.impact.2023.100476>

Received 4 January 2023; Received in revised form 17 May 2023; Accepted 4 July 2023

Available online 10 July 2023

2452-0748/© 2023 The Authors. Published by Elsevier B.V. This is an open access article under the CC BY license (<http://creativecommons.org/licenses/by/4.0/>).

(David et al., 2016). However, the full extent to which MWCNT exposure phenotypes are altered by their structural properties remains unknown and requires further investigation.

Previous work has demonstrated that MWCNTs induce altered macrophage cytokine and chemokine signaling at sublethal levels (Meng et al., 2015; Dong and Ma, 2018a; Kinaret et al., 2020), implicating them as potential immunotoxins in the progression of MWCNT related pathogenesis. In the lungs, macrophages are among the first responders to epithelial insult by foreign substances. Persistent damage to the bronchial and alveolar epithelium signals the recruitment of monocytes that, after activation and differentiation to macrophages, work together with tissue resident macrophages, eosinophils, neutrophils and myofibroblasts, to resolve the damage, and attempt clearance of the initial insult (Wendisch et al., 2021; Adler et al., 2020). Macrophage pattern recognition receptors (e.g. toll-like receptors) activate downstream signaling pathways upon direct interaction with foreign substances, and alter the behavior of macrophages toward clearing out foreign substances via phagocytosis (David et al., 2016; Sharma et al., 2016). However, with fiber-like particles this clearance can be insufficient, leading to the induction of proinflammatory cytokines IL1B and TNF and eventually profibrotic signals including TGF β (Sharma et al., 2016). For moderate non-repetitive epithelial injury, TGF β drives profibrotic signals inducing tissue healing, but this same profibrotic environment, after repeated injury can lead to excessive fibroblast activation and collagen production causing thickening and scarring of the alveolar wall, fibrosis and impaired gaseous exchange and diminishing lung capacity (Sharma et al., 2016; Dong and Ma, 2018b; Wynn, 2008).

The immune regulatory microenvironment changes seen upon MWCNT exposure, along with the aforementioned roles of macrophages in attempts at clearing MWCNTs, merits the study of direct macrophage exposure to MWCNTs in an in vitro system. Proinflammatory cytokines are secreted rapidly, and their modes of regulation reflect this. IL1B precursors are kept at a primed level within macrophages, and TNF mRNA is constantly produced for expedient translation when necessary (Murray and Stow, 2014). These rapidly secreted proinflammatory cytokines mediate an innate immune response by recruiting and activating phagocytic cells, eventually inducing an adaptive immune response. On the other hand, anti-inflammatory cytokines such as IL4, IL10 and IL13, suppress proinflammatory responses by inhibiting proinflammatory cytokine secretion and their downstream signaling, whilst also inducing the secretion of growth factors and recruiting fibroblasts (Murray and Stow, 2014; Ott et al., 2007). The secretion of cytokines has great potential in studying the immunotoxicity of MWCNTs, as it is one of the fastest acting mechanisms in the immune system (Dietert and Holsapple, 2007; Elsabahy and Wooley, 2013), allowing for analysis on time scales compatible with in vitro studies.

Finally, traditional approaches to toxicology and chemical hazard assessment use phenotypic endpoints to qualify exposures as harmful, but this falls short of elucidating the underlying mechanism of action (MOA) (Joseph, 2017). The nascent field of systems toxicology seeks to go further by interpreting underlying pathways involved in reaction to the initial toxic insult, employing OMICs methodologies and in silico models. Transcriptomics has been used to explore gene expression changes in response to MWCNT exposure (Kinaret et al., 2020; Horstmann et al., 2021; Scala et al., 2021), but these studies have not explored the direct correlation of gene expression to the associated cytokine secretion profiles.

As demonstrated by a lineage tracing experiment in mice, deletion of monocyte derived alveolar macrophages ameliorated bleomycin induced lung fibrosis, which was not the case when tissue resident macrophages were deleted (Misharin et al., 2017). This is consistent with studies showing that the depletion of circulating monocytes (e.g. in Ccr2^{-/-} mice), also limits the severity of lung fibrosis (Moore et al., 2001; Ogawa et al., 2021). Therefore, recruited monocytes that differentiate into macrophages at the site of injury are crucial to the immune response during the progression of lung fibrosis. In this study, we utilize

an in vitro monocyte model differentiated into macrophages, comparable to recruited bone marrow derived monocytes (Chanput et al., 2014; Bosshart and Heinzlmann, 2016; Tsuchiya et al., 1980), to scrutinize immunotoxicity upon exposure to a set of 7 MWCNTs, differing in surface area, aspect ratio and structure (rigid vs. tangled). We measure a panel of 10 cytokines, including both pro- and anti-inflammatory cytokines, to give precise information on the signaling status of macrophages. Our results indicate tangled MWCNTs induce dose-dependent IL1B pro-inflammatory cytokine secretion, which was not observed with rigid MWCNTs. Taking a systems toxicology approach, we investigated the MOA of MWCNT through transcriptomics analysis of dose-dependent gene expression. We found dose dependent alterations in gene expression, showing that all 7 MWCNTs cause gene expression dysregulation in crucial signaling pathways, including metabolism and the immune system. By combining data on altered gene expression with observed cytokine secretion changes into a multilayer model, we were able to link MWCNT structure to differences in pattern recognition related pathways, which were enriched by tangled but not by rigid MWCNTs. The multilayer analysis also showed a spectrum of gene expression changes induced by MWCNTs, correlating to either pro-inflammatory or anti-inflammatory cytokines. By coupling transcriptomics profiling with cytokine secretion, we gained mechanistic information on where differences are arising in immunotoxic outcomes from MWCNT exposure, that traditional toxicological hazard assessment studies would fail to observe.

2. Materials and methods

2.1. Nanomaterials

All nanomaterials used in this study were MWCNTs. These materials have been characterized in NanoAtlas (Vippola et al., 2009) or in the case of NM400 and NM401 by the joint research center (Rasmussen et al., 2014). Their properties are summarized in Table 1.

2.2. THP-1 cell culture

THP-1 cells (ATCC TIB-202, USA) were cultured in RPMI-1640 (Gibco, USA) supplemented with 10% FBS (Gibco, USA) (culture media). Cells were cultured in 75 cm² flasks at a density < 1 × 10⁶ cells/ml. Cells were differentiated in 12 well plates, with 150,000 cells/well (39,474 cells/cm²), in the culture media supplemented with 25 nM of phorbol 12-myristate 13-acetate (PMA) (Sigma-Aldrich, USA) for 48 h. After PMA differentiation, cells rested for 24 h in 500 μ l of RPMI-1640 supplemented with 1% FBS (exposure media) before MWCNT exposures.

2.3. MWCNT dispersions

A stock solution of each MWCNT was prepared on the day of the exposure following the method in Scala et al. (Scala et al., 2018). Briefly, for powdered MWCNTs, a 1 mg/ml stock solution in exposure media, in glass tubes was prepared. NM400 and NM401, originally in water at 1 mg/ml, were diluted 1:1 in 2% FBS RPMI-1640, for a final 0.5 mg/ml stock solution in 1% FBS RPMI-1640. Each of the stock solutions was sonicated in a bath sonicator for 2 x (BAY, CHT, SES, SIG) or 3 x (MIT, NM400, NM401) 15 min at 37 °C, with vortexing after each sonication, prior to use.

2.4. WST-1 cytotoxicity assay

An initial test to see whether the MWCNTs interfered with the WST-1 assay was performed. 100 μ g/ml of SIG with and without cell proliferation reagent WST-1 (Roche, #11644807001) and with and without THP-1 cells were plated and scanned from 350 to 1000 nm, with WST-1 reagent only and cells only used as a control. The scan indicated that there is no interference with the emission coming from WST-1 and with

Table 1
Properties of MWCNTs.

Acronym	Manufacturer	Physical state	Length (nm)	Diameter (nm)	Surface area (m ² /g)	Aspect ratio	Structure	Source
MIT (XNRI MWNT-7, MWNT-7, NRCWE- 006)	Mitsui & Co.	Powdered	13,000	50	22	260	Rigid	(Vippola et al., 2009)
NM401	JRC repository	1 mg/ml In H ₂ O	4048 ± 2371	67 ± 24	30.5	60	Rigid	(Rasmussen et al., 2014)
SIG	Sigma-Aldrich	Powdered	100,000	15	567	6666	Rigid	(Vippola et al., 2009)
SES	SES research	Powdered	1500	20	60	75	Tangled	(Vippola et al., 2009)
CHT	Cheaptubes Inc.	Powdered	30,000	11.5	180	2608	Tangled	(Vippola et al., 2009)
NM400	JRC repository	1 mg/ml In H ₂ O	846 ± 446	11 ± 3	189.3	77	Tangled	(Rasmussen et al., 2014)
BAY	Bayer material science	Powdered	1000	14.5	204	69	Tangled	(Vippola et al., 2009)

SIG in the wavelength used to measure WST-1 signal (540 nm) (Fig. S1).

To calculate IC₅, IC₁₀ and IC₂₀ concentrations for each MWCNT, THP-1 cells were exposed to 8 concentrations of MWCNT in a two-fold dilution series ranging from 100 to 0.78 µg/ml, in four replicates. For each MWCNT-concentration, a blank containing exposure media and MWCNT alone was used. Unexposed cells were used as negative control. Cells were exposed for 24 h, after which the WST-1 assay was performed by adding 10 %V/V of WST-1 reagent into each well and incubating for 2 h 15 min. The WST-1 emission was then measured at 450 nm with a multiplate reader Spark (Tecan). The cytotoxicity assay was repeated three times for each nanomaterial.

After subtracting the blank values for each concentration of MWCNT, IC-values were calculated using a three-parameter nonlinear regression model in GraphPad Prism 9 for Windows (GraphPad Software, USA).

2.5. Sample collection for multiplex ELISA and DNA microarray

For multiplex ELISA and DNA microarray assays THP-1 cells were seeded in 2 × 12 well plates, and exposed in replicates of 6, to IC₅, IC₁₀ and IC₂₀ concentrations, calculated by WST-1 assay (see section 2.4). Exposures were performed in a semi-random distribution, with 4 negative controls (unexposed cells) per MWCNT. Cells were exposed for 24 h. Supernatant for multiplex ELISA and cell lysate for RNA isolation, were collected from the same well. For both assays, two wells were pooled, per concentration, for a final of 3 replicates per MWCNT exposure and 2 replicates of negative controls per MWCNT.

2.6. Multiplex ELISA

For multiplex ELISA from the collected supernatants (see section 2.5) a V-PLEX Proinflammatory Panel 1 Human Kit (Meso Scale Diagnostics, USA) containing 10 probes for cytokines IFNG, IL1B, IL8, IL6, IL12, TNF, IL2, IL4, IL10 and IL13 was used. The assay was performed following vendor's instructions. The raw data from multiplex ELISA is in Table S1 and the full range of cytokine secretion is shown in Fig. S2.

2.7. DNA microarray

Cells were lysed on the plate and RNeasy mini kit (Qiagen, Germany) was used as per the vendor's instructions. The quality of the RNA samples was verified using Bioanalyzer 2100 (Agilent, USA), with RNA 6000 Nano Kit (Agilent, USA) following vendor's instructions. The RIN values for each sample exceeded 9.4.

DNA microarray was performed following the T7 RNA polymerase amplification protocol provided by Agilent Technologies (USA). Briefly, for amplification and labeling of RNA samples, Two Color Low Input Quick Amp Labeling Kit (Agilent, USA) was used, in which cRNA

samples were labeled either with Cy3 or Cy5 dyes. The labeled cRNA samples were purified using RNeasy Mini Kit (Qiagen, Germany) and the quantity and specific activity was verified with NanoDrop ND-2000 (Thermo Fisher Scientific, USA). Equal masses of Cy3 and Cy5 labeled samples were combined and the samples were fragmented and hybridized onto Agilent SurePrint G3 Human GE 8 × 60 microarrays slides. Finally, the slides were washed and scanned with Agilent microarray scanner G2505C (Agilent, USA). The data was extracted using Agilent Feature Extraction software (version 12.2.2, Agilent, USA). All of the samples were randomly distributed across slides and labeling colors were randomly selected for each sample. DNA microarray data has been submitted to NCBI Gene Expression Omnibus (GEO) database, under series accession number GSE220646.

2.8. Transcriptomics preprocessing and differential gene expression

The preprocessing and differential gene expression analysis of the DNA microarray data was performed using the eUTOPIA application (Marwah et al., 2019). Raw data was imported, and low-quality probes were filtered out using a quantile based cutoff, in which probes with intensities higher than the 80% quantile of negative control probes in at least 80% of the samples remained for further steps. Log₂ transformed values were normalized between arrays using the quantile normalization method. The ComBat method, from the sva R package (Leek et al., 2012) was used to remove the technical variation induced by slides and labeling dyes. The probes mapped to the same gene symbol were aggregated by their median values and annotated using the GLP20844-88004 annotation file retrieved from Agilent eArray (<https://earray.chem.agilent.com/earray/>).

Differentially expressed genes were retrieved for each MWCNT separately by comparing each dose against the controls. This analysis was performed in eUTOPIA by means of the R-package limma (Ritchie et al., 2015). Genes with nominal *p*-value above 0.05 were not considered differentially expressed.

2.9. Dose-dependent analysis of transcriptomics and multiplex ELISA

The BMDx application (Serra et al., 2020) was used to identify lists of dose-dependent genes and cytokines. To retrieve the dose-dependent genes, the annotated and aggregated transcriptomics data processed with eUTOPIA was imported in BMDx along with the corresponding phenotype data. The benchmark dose modeling was performed under the assumption of constant variance and a benchmark response factor (BMR) set to 1.349. For each gene, multiple models were fitted including linear, second order polynomial, power 2, exponential, hill, three- and two-parameters log-logistic model, two-parameters Weibull model, two-parameters Asymptotic regression model, and two-

parameters Michaelis-Menten model. Models with lack-of-fit p -values lower than 0.1 were removed from the analysis. Finally, if multiple models were fitted for a gene, only the model with the lowest Akaike Information Criterion (AIC) value was used to estimate the BMD values. Genes for which the BMDx tool was not able to estimate the effective BMD values were further removed from the analysis.

The same analysis was repeated with the multiplex ELISA data to retrieve the dose-dependent cytokines. Cytokines for which a BMD-value could not be determined were not filtered out, because we were only interested in checking whether the dose-dependent trend was present. Only the models with R^2 above 0.5 were used in the final results. If multiple models were fitted to the same cytokine, the one with the highest R^2 was selected.

2.10. Multilayer correlation analysis

The Pearson correlation across the range of MWCNT doses, using stats R package, was calculated for signal from multiplex ELISA against fold-changes from genes which were both dose-dependent and differentially expressed. Correlations with p -value above 0.05 were discarded. The correlation coefficient and p -values for each cytokine-gene comparison for each MWCNT are provided in Tables S2 and S3.

2.11. Enrichment analysis

FunMappOne application can be used to visualize enrichments of multiple experiments in 3-level hierarchical systems from least to most specific (Scala et al., 2019). This application was used in two assays, to investigate the functional roles of 1) dose-dependent genes and 2) dose-dependent and differentially expressed genes correlating with cytokine secretion. Functional annotation was done against REACTOME terms. Mean summarization function was used with gSCS p -value correction, with the p -value threshold set at 0.05. The enrichment for 43 common differentially expressed genes.

3. Results and discussion

THP-1 macrophages were used to analyze the immunotoxic potential of 7 MWCNTs, using a multiplex ELISA cytokine secretion analysis, and a DNA microarray transcriptomics analysis, and finally correlating data from these two experiments in a multilayer analysis revealing mechanisms of MWCNT immunotoxicity. An overview of the workflow used in this study can be seen in Fig. 1.

3.1. Short, rigid MWCNTs are cytotoxic at low concentrations

Cytotoxicity has the potential to mask the signatures of sublethal exposures in toxicological assays that aren't using cytotoxicity as an endpoint. When cells are dying they are inducing major alterations in gene-expression, signaling and morphology (Fiers et al., 1999), which can cause interference when measuring, for example, immunotoxicity outcomes at the level of cytokine signaling. In order to prevent masking of potential immunotoxic effects in our downstream analyses, we first used a cytotoxicity assay to determine equipotent sublethal doses of MWCNTs to be used in follow up experiments. To achieve adequate exposures of MWCNTs to the adherent THP-1 cells, a time point of 24 h post-exposure was selected for analysis, based on previous studies of the sedimentation rate of MWCNTs (Septiadi et al., 2019; Bihari et al., 2008). The cytotoxicity of THP-1 cells when exposed to 7 different MWCNTs (Table 1) was measured using WST-1 reagent solution (Fig. 2), which, importantly, did not itself interact with the MWCNTs based on our measurements (Fig. S1).

MIT, NM401 and NM400 were the most cytotoxic by concentration, with an IC_{50} in each case ≤ 8.1 $\mu\text{g}/\text{ml}$, while CHT was the least cytotoxic with an IC_{50} of 59.8 $\mu\text{g}/\text{ml}$ (Fig. 2). Rigid materials (MIT, NM401, SIG) were systematically more cytotoxic than tangled materials (NM400, BAY, SES, CHT) with the exception of NM400, which was slightly more cytotoxic than SIG (Fig. 2). Furthermore, within the tangled MWCNTs, shorter length correlated with greater cytotoxicity. Meaning that although the longest and the shortest of the tangled MWCNTs (NM400 and CHT) had similar surface areas, the length still affected the

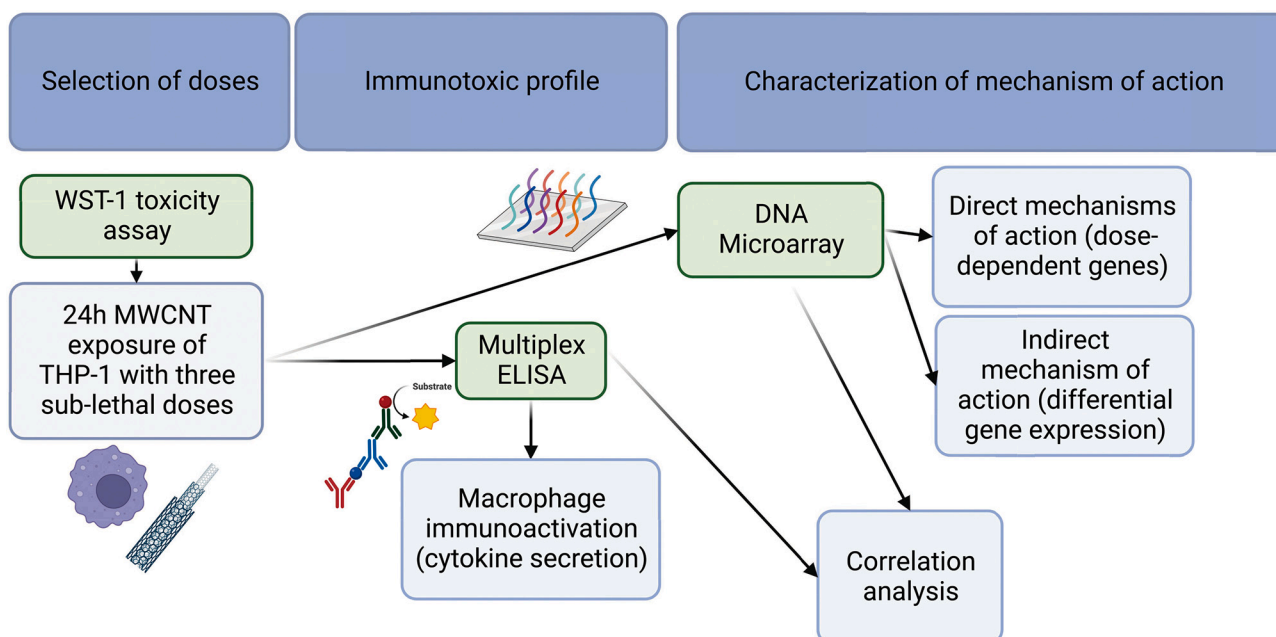


Fig. 1. Overview of the workflow. Selection of sublethal doses was done with a WST-1 viability assay for each of the MWCNTs. A 24 h MWCNT exposure at cytotoxicity IC_5 , IC_{10} and IC_{20} concentrations was performed, followed by multiplex ELISA assay to discover cytokine secretion profiles and the immunotoxicity of each MWCNT. DNA microarray transcriptomics was used to characterize the mechanism of action of MWCNTs. Finally, the transcriptomics and secretion profiles were combined into a multi-layer model via correlation analysis to discover inflammatory profiles and to investigate mechanism of action of cytokine mediated immunotoxicity with different MWCNTs. Figure created with Biorender.com.

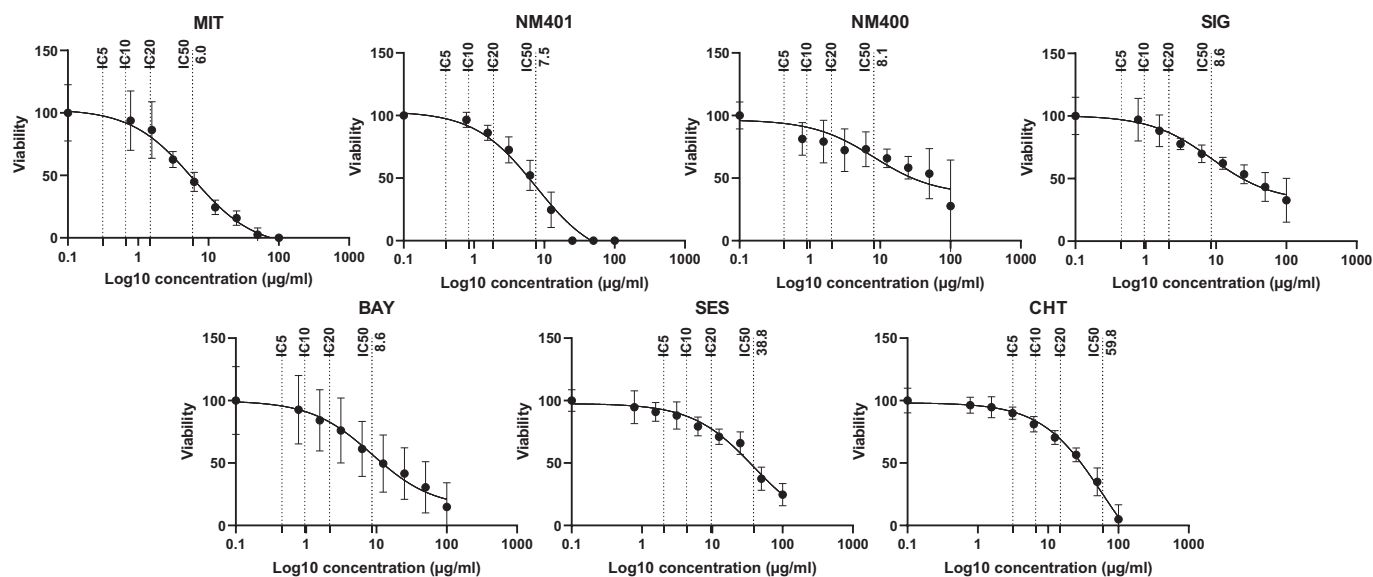


Fig. 2. Cytotoxicity of MWCNTs measured using WST-1 viability assay. IC50 concentrations are indicated. MWCNTs are ordered from most to least cytotoxic.

properties of MWCNTs enough to cause differential THP-1-MWCNT interactions. Within the rigid materials, the longest, SIG, was also the least cytotoxic. This suggests a possible correlation between MWCNT length and cytotoxicity, where the shorter MWCNTs used here are more cytotoxic, which could be due to greater rates of internalization (Sohaebuddin et al., 2010). The toxicity of MWCNTs has often been linked to the amount of their active surface area (Joris et al., 2013). By transforming the concentrations used in the WST-1 assay into surface area/volume or surface area/cm² concentrations, we still observe that the order from most to least cytotoxic MWCNT remains the same, with the exception of SIG, which becomes the second to last cytotoxic (Table S1). Similar to our findings in THP-1 cells (Fig. 2), thin and rigid materials induced greater cytotoxicity in mesothelial cells as compared to tangled materials (Nagai et al., 2011; Hamilton et al., 2013). Thin and rigid materials have also been observed to cause greater in vivo inflammogenicity and to have more fibrotic potential (Nagai et al., 2011). Strict comparisons between MWCNT in vitro cytotoxicity assays is challenging due to the heterogeneity between experimental setups, concentrations used and different MWCNTs used.

By using equipotent concentrations of MWCNTs for immunotoxicity assays we can avoid masking the effects of MWCNT structural properties by intracellular, paracrine and autocrine signals caused by high levels of cytotoxicity. Based on the results of our WST-1 assay (Fig. 2), we determined IC5, IC10 and IC20 concentrations (Table S4), to be used in follow up experiments, as these concentrations did not induce major cell death but did differ from the baseline viability. These concentrations range from 0.3 to 15 µg/ml (0.08 µg/cm² to 3.9 µg/cm²) (Table S4). Lifetime occupational exposure to MWCNTs has been estimated to be between 10 and 50 µg/cm² (Gangwal et al., 2011). Thus our exposures in the following assays can be said to be within the limits of human relevant concentrations.

3.2. Tangled MWCNTs induce dose-dependent IL1B secretion

Immunotoxicity of the MWCNTs, based on cytokine signaling, was measured using a multiplex ELISA assay. The cytokine panel included both proinflammatory; IL1-beta (IL1B), IL6, IL8, IL12, TNF-alpha (TNF) and interferon gamma (IFNG) and anti-inflammatory; IL2, IL4, IL10 and IL13 cytokines (Bou Zerdan et al., 2021; Banchereau et al., 2012; Zhang and An, 2007). These cytokines have previously been suggested as useful quantitative indicators of nanoparticle immunotoxicity (Elsabagy and Wooley, 2013). An MWCNT was defined as immunotoxic if it caused

dose-dependent cytokine secretion from THP-1 macrophages. That is, the MWCNT has the potential to lead to adverse outcomes by directly changing immune regulatory activity. By placing significance specifically on dose-dependently secreted cytokines we only observe cytokine secretion changes that are a direct consequence of MWCNT exposure (Fig. 3).

Of the 7 MWCNTs we analyzed, MIT and SIG did not induce any dose-dependent cytokine secretion (Fig. 3). Our results indicate BAY, CHT, NM400, NM401 and SES to have immunotoxic potential at sub-lethal doses (Fig. 3). The proinflammatory cytokines increased in a dose dependent manner by MWCNT exposure were IL1B and IL6 (Fig. 3). Most notably, IL1B was strongly increased in a dose-dependent manner by tangled MWCNTs (NM400, BAY, SES, CHT) and not by rigid MWCNTs (NM401, MIT, SIG) (Fig. 3). IL10 and IL13 were the only anti-inflammatory cytokines seen to respond dose-dependently to MWCNT

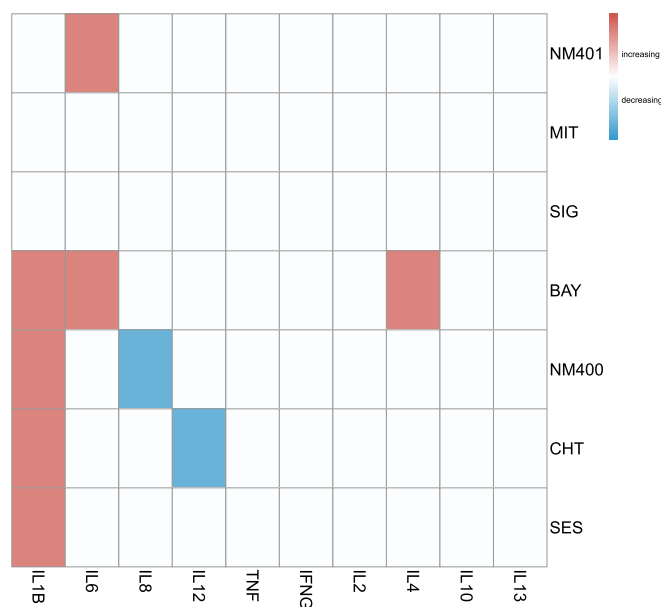


Fig. 3. Cytokines secreted in a dose-dependent manner for each of the MWCNTs. Color indicates whether the secretion is dose-dependently increasing (red) or decreasing (blue). (For interpretation of the references to color in this figure legend, the reader is referred to the web version of this article.)

exposure, with IL10 decreasing with NM400 exposure, while IL13 was increased with BAY exposure (Fig. 3). The non-immunotoxic MWCNTs, MIT and SIG, were rigid MWCNTs with the highest aspect ratio and length (Table 1). MWCNT aspect ratios and length are, therefore, critical determinants of cytokine secretion in exposed macrophages, and IL1B secretion is an important immunotoxic effect seen with exposure to tangled MWCNTs.

Previous studies have also investigated the secretion of cytokines and changes in gene expression, with macrophages, in relation to MWCNT characteristics. PMA and LPS treated THP-1 cells were found to induce higher secretion of IL1B when exposed to MWCNTs with small diameter and large length for 24 h (Hamilton et al., 2013). Similarly, long MWCNTs have been found to induce a greater release of acute proinflammatory cytokines and chemokines (IL1B, TNF, IL6 and IL8) from THP-1 cells when compared to short MWCNTs, with the implication that longer CNTs causing frustrated phagocytosis leads to a greater proinflammatory response (Murphy et al., 2012). The unstandardized approach of current assays in the field, using varied concentrations of MWCNT makes comparison of different in vitro assays difficult, further supporting a need for robust, standardized, and validated immunotoxicity assays. By using IC values to determine equipotent sublethal exposure concentrations, analyzing MWCNTs with varied structural properties, and by measuring a large panel of cytokines for MWCNT dose-dependent response, the approach followed here can act as a base for future standardized in vitro assays analyzing MWCNT immunotoxicity. To understand the MOA underlying the immunotoxic potential of MWCNTs in more detail, we proceeded to perform transcriptomics analysis of THP-1 cells exposed to MWCNTs.

3.3. Signal transduction and immune system pathways are dysregulated by MWCNT exposure

To further understand the MOA of the 7 MWCNT structures in immunomodulation, a transcriptomics assay was performed on RNA isolated from exposed THP-1 macrophages. Three methods were used to

identify genes that are playing a role in the MOA of MWCNT exposure: 1) analysis of dose-dependently altered genes, 2) analysis of differentially expressed genes, and 3) the identification of genes whose expression correlates with cytokine secretion (Fig. 4). Genes not included in these categories were deemed unaltered by MWCNT exposure (Fig. 4 and Fig. S3 light gray). The correlation analysis against cytokines also identified genes correlating with unaltered cytokines, thus a subset of the genes in this category are unaltered in their mRNA expression (Fig. 4 dark gray).

With each individual MWCNT exposure, the number of genes falling into these categories varied (Fig. 5). MIT exposure gave the highest total number of dose-dependent genes (Fig. 5), while irrespective of dose-dependence, SIG exposure caused the highest number of differentially expressed genes (Fig. 5). Analysis of differentially expressed genes showed that many of the altered genes did not change in a dose-dependent manner, but instead expressed non-monotonic alteration (Fig. 5). All 7 MWCNTs commonly induced differential expression of 43 genes (Fig. S6). These genes were enriched in signal transduction related terms such as MAPK, RAS, NOTCH and growth factor related pathways (Fig. S7). Corresponding with diseases that arise from MWCNT exposure, these pathways are often implicated in oncogenesis and lung diseases such as pulmonary fibrosis (Braicu et al., 2019; Yang et al., 2021; Stella et al., 2022). The internalization of MWCNTs has previously been shown to occur in part through endosomal and vacuolar routes (Manzanares and Ceña, 2020; Foroozandeh and Aziz, 2018), and endosomal/vacuolar pathways are enriched in these 43 common genes (Fig. S6) potentially suggesting a common route of internalization for each of the MWCNTs used here.

Differentially expressed genes includes indirectly altered genes whose expression is either downstream in relevant signaling pathways, or subject to regulatory feedback. Therefore, we also used dose-dependent analysis to identify genes whose expression is altered directly by MWCNT exposure (Serra et al., 2020), with the number of dose-dependent genes being linked to the magnitude of effect induced by an exposure (Serra et al., 2020; Gao et al., 2015; Gou et al., 2010;

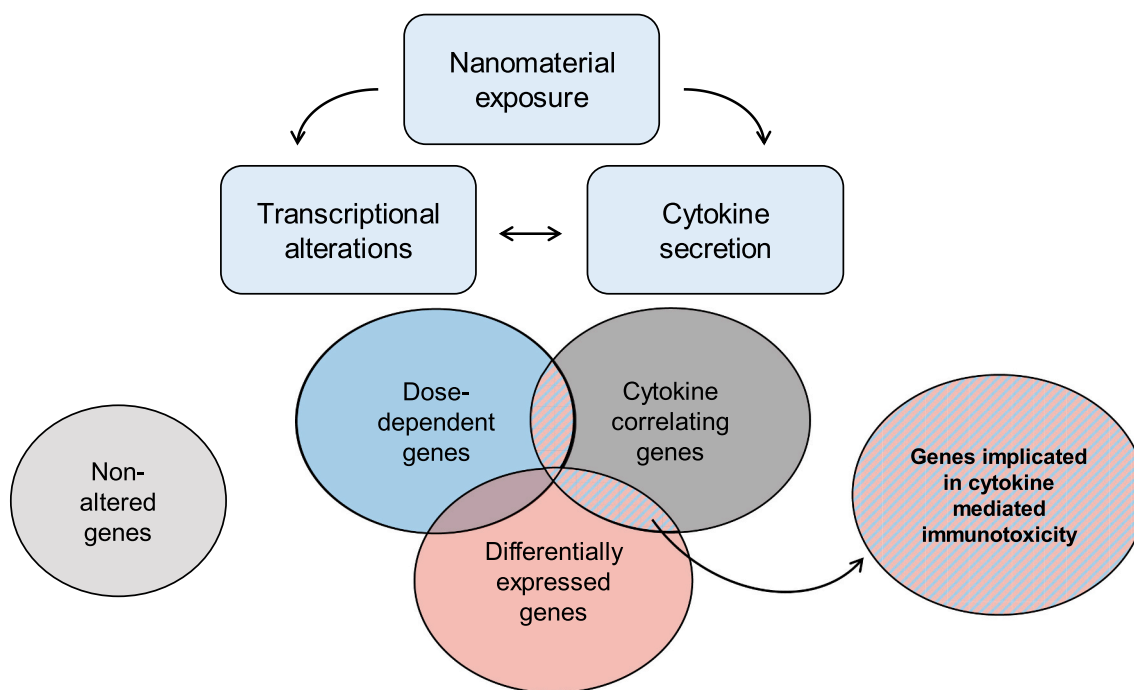


Fig. 4. An overview of transcriptional and cytokine secretion alterations induced by MWCNT exposure. BMD modeling revealed dose-dependent genes, which had direct correlation to the MWCNT concentration. Analysis of differentially expressed genes also revealed genes with non-monotonic transcriptional alterations. A subset of genes correlated with cytokine secretion, which include genes affecting cytokine secretion and genes altered by cytokines (autocrine effects). We identified that the altered genes correlating with cytokine secretion were the essential genes in cytokine mediated immunotoxicity.

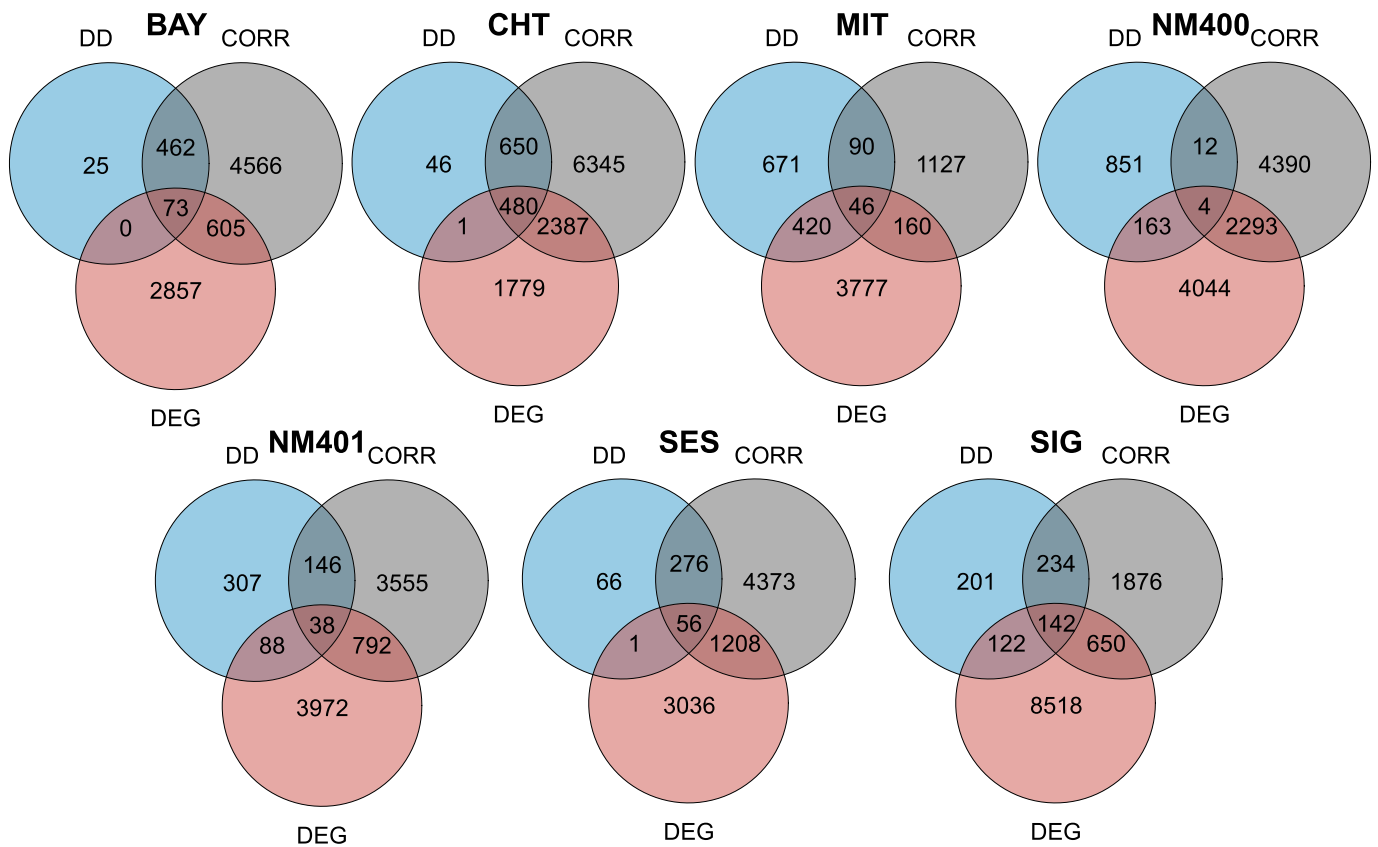


Fig. 5. Venn-diagrams of dose-dependent genes, differentially expressed genes and genes correlating with cytokines for each MWCNT. DD = dose-dependent, DEG = differentially expressed genes, CORR = correlating with cytokines.

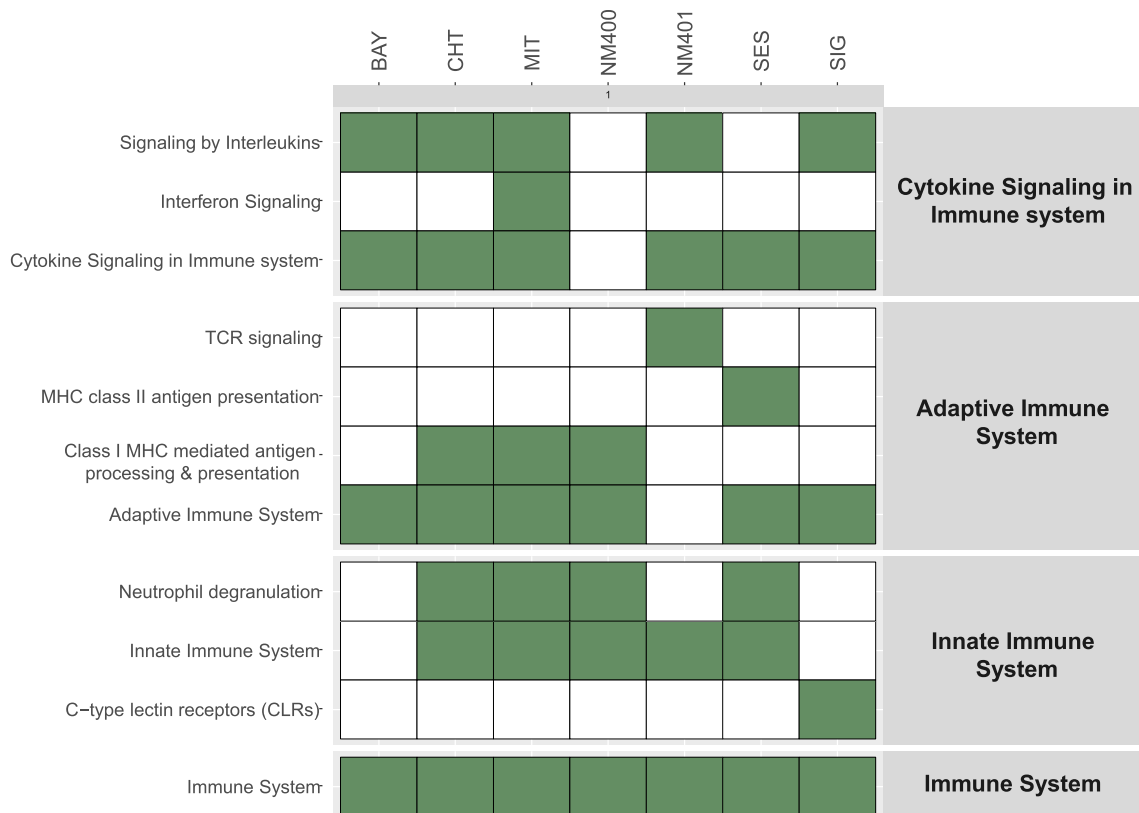


Fig. 6. Enrichment of dose-dependent genes against immune system related REACTOME terms.

Hockley et al., 2006; Yang et al., 2007). Going by this measure, MIT with the highest number of dose-dependent genes, was the most potent of the MWCNTs, followed by CHT, NM400, SIG, NM401, BAY and SES (Fig. 5). Given this, it is unsurprising that MIT and NM400 had low IC50 values and were more cytotoxic (Fig. 2). While further examination revealed no dose-dependently altered genes were shared by all of the MWCNTs (Fig. S4), exploration of functional roles of these genes revealed commonalities between the MWCNTs (Fig. S5). Of the enrichments on the highest level of REACTOME term hierarchy common terms for all MWCNTs were: developmental biology, metabolism, signal transduction, cell cycle, disease and immune system, protein metabolism, vesicle-mediated transport, gene expression and RNA metabolism (Fig. S5). Due to our findings on MWCNT induced cytokine secretion and immunotoxicity (see section 3.2), we looked closer at immune system related terms (Fig. 6).

Of the innate immune system related terms, neutrophil degranulation was enriched by all but NM401, SIG and BAY (innate immune system was not enriched at all by SIG and BAY) (Fig. 6). Upon activation, macrophages can recruit neutrophils which use degranulation as a method of eliminating foreign intruders, however this may also lead to tissue damage (Prame Kumar et al., 2018; Lacy, 2006). Innate immunity mediated lung damage, linked to neutrophil and eosinophil influx, has been shown in vivo to induce cellular damage without activation of the adaptive immune system (Loret et al., 2022). The observed enrichment of degranulation may therefore be relevant to in vivo cell damage caused as a result of an innate immune reaction to MWCNTs. Induction of an innate immune reaction has been linked to high surface area and rigidity of carbon nanotubes (Rydman et al., 2014; Liu et al., 2017). However, we did not see a clear correlation between immune system related term enrichment and the structural characteristics of the MWCNTs tested here.

We also investigated how the genes coding for cytokines used in the immunotoxicity assay (see section 3.2) are modulated by MWCNT exposure at the mRNA level. None of the cytokine coding genes were dose-dependently expressed, however some of them were differentially expressed (Fig. S8). Of note, many of these cytokine coding genes were found to have negative fold change in mRNA expression compared to the control (Fig. S8). For example, while CHT, NM400 and SES induced increasing dose dependent IL1B secretion (Fig. 3), *IL1B* RNA expression was decreased by exposure to these MWCNT (Fig. S8), likely indicating a negative feedback mechanism. We also found SIG, which did not induce dose-dependent cytokine secretion (Fig. 3), did dose-dependently decrease *CXCL8* mRNA expression (Fig. S8), but this effect was not strong enough to cause alterations in the cytokine secretion microenvironment, or then the effect of decreased mRNA was not reflected in secreted IL8 at 24 h. Because cytokines can have constant mRNA production or are stored in the cells as pro-cytokines, their secretion does not necessarily require or reflect changes at the mRNA level (Murray and Stow, 2014; Ott et al., 2007).

Overall, through transcriptomics analysis, we observed a high variation in the genes altered by different MWCNTs indicating that the MOA leading to the adverse effects of MWCNT exposure is affected by the intrinsic properties of MWCNTs. However, no clear correlation between a specific intrinsic property of MWCNTs and mRNA expression was detected. The different transcriptome profiles observed upon MWCNT exposure are therefore most likely determined by a combination of the underlying MWCNT structural characteristics. We proceeded by integrating altered gene expression data with cytokine secretion data into a multilayer model.

3.4. A multilayer analysis of MWCNT exposure reveals mechanisms of immunotoxicity

We reasoned that the gene subsets relevant to MWCNT immunotoxicity could be further refined by looking for those genes whose RNA expression correlates with measured cytokine secretion. Therefore,

cytokine secretion and transcriptomics results were brought together into a multilayer analysis to see if this could reveal mechanisms of immunotoxicity induced by MWCNT exposure that aren't seen by analyzing dose-dependently and differentially expressed genes.

As with the amount of dose-dependent genes being used as an indication of the potency of each MWCNT exposure (Serra et al., 2020; Gao et al., 2015; Gou et al., 2010; Hockley et al., 2006; Yang et al., 2007), the number of genes correlating with cytokine secretion can be used to indicate the immunomodulatory potency of the exposure, and filters out many genes that are differentially or dose-dependently expressed but not directly involved in the immune response of the macrophages. Based on this, CHT was found to have the highest immunomodulatory potency followed by NM400, SES, BAY, SIG, NM401 and MIT (Fig. 5). This result highlights a clear difference between rigid and tangled MWCNTs, where tangled MWCNTs have higher immunomodulatory potency than rigid materials. It is possible that this is linked to the increase in IL1B secretion caused by tangled MWCNT exposure (Fig. 3) and that the increased immunomodulation seen with tangled MWCNT exposure is what protects the macrophages from the higher rates of cytotoxicity at higher concentrations when compared to the increased cytotoxicity of rigid MWCNT exposure (see section 3.1). Corroborating our initial cytokine secretion results (Fig. 3), the number of cytokine correlating genes is low with the MWCNTs not inducing dose-dependent cytokine secretion, with 1127 and 1876 correlating genes found for MIT and SIG respectively, as compared to >3000 cytokine correlating genes for the other MWCNTs (Fig. 5), again suggesting that MIT and SIG are less immunotoxic when compared to the other MWCNTs.

Each MWCNT gives a unique profile regarding the proportion of genes correlating to each cytokine (Fig. 7). MWCNTs were deemed more or less proinflammatory based on the percentage of the altered genes correlating with pro- or anti-inflammatory cytokines (Fig. 7). While seen to be less immunotoxic along with MIT based on low numbers of cytokine correlating genes, SIG was the only MWCNT without any genes correlating with anti-inflammatory cytokines and instead correlating primarily with TNF, giving the most proinflammatory profile of all MWCNTs (Fig. 7). At the other end of the spectrum, NM400 had the highest percentage of genes correlating with anti-inflammatory cytokines (Fig. 7). Across all MWCNTs, cytokine correlating genes were mainly correlating with proinflammatory cytokines (Fig. 7) suggesting exposure to MWCNTs over 24 h primarily causes a proinflammatory response by macrophages. The order from most to least proinflammatory profiles correlated with length of the material (Fig. 7), whereby the longest MWCNTs induced a more proinflammatory profile than shorter materials (Fig. 7). Previous studies have also suggested long MWCNTs as more proinflammatory when using cytokines as a measure for inflammogenicity (Hamilton et al., 2013; Murphy et al., 2012; Donaldson et al., 2010). In a comparison between dose-dependent cytokine secretion and inflammatory profiles, all of the MWCNTs were found to correlate with the cytokines which they were causing macrophages to dose-dependently secrete (Fig. 3 & Fig. 7), supporting the use of this novel multilayer analysis to identify MWCNT immunomodulatory effects. For example all of the materials inducing dose-dependent IL1B secretion (BAY, NM400, CHT, SES), were also found to have a significant percentage of altered genes correlating with IL1B secretion (Fig. 3 & Fig. 7).

To understand the functional roles of the altered genes associated with the cytokine polarization profiles, enrichment analysis was performed (Fig. S9). Enriched terms shared by all MWCNTs were signal transduction and immune system once again supporting this multilayer analysis approach as a means of observing MWCNT exposure immunomodulation potential (Fig. S9). Tangled MWCNTs but not rigid gave the enrichment terms programmed cell death, vesicle-mediated transport, metabolism of RNA and cellular response to external stimuli (Fig. S9). Looking further at these terms at another layer of enrichment, only tangled MWCNTs gave the following enrichment terms: TLR-receptor cascade, Class 1 MHC mediated antigen processing and presentation,

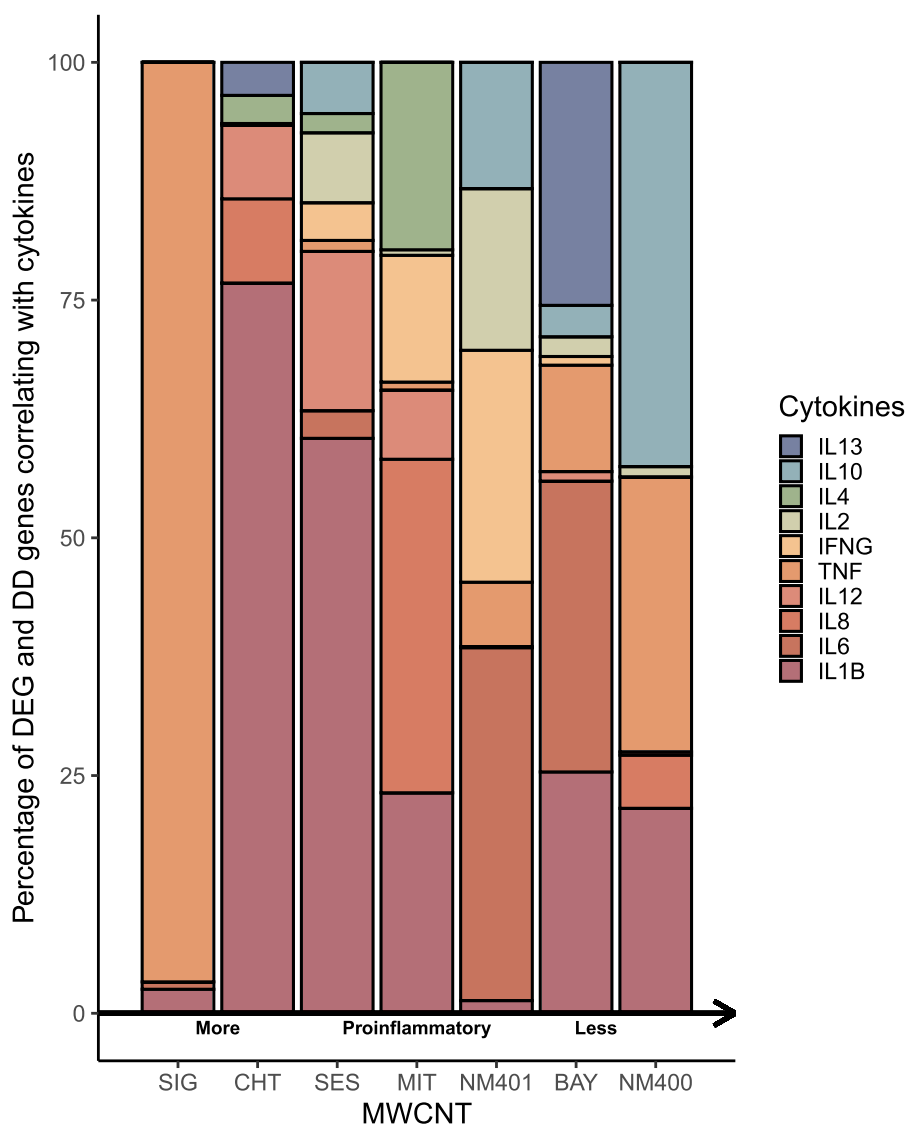


Fig. 7. Percentage of genes correlating with each of the studied cytokines represents the inflammatory profiles induced by different MWCNTs. IL13, IL10, IL4 and IL2 are considered anti-inflammatory cytokines while IFNG, TNF, IL12, IL8, IL6 and IL1B are proinflammatory cytokines.

intracellular signaling by secondary messengers, MAPK, WNT and receptor tyrosine kinase signaling pathways, macroautophagy and membrane trafficking (Fig. S9). Of particular note, many of these terms are related to pathways which are used in recognition and internalization of MWCNTs (David et al., 2016; Halappanavar et al., 2020). MHC class I antigen presentation leads to activation of cytotoxic CD8-positive T-cells (Kim et al., 2019). For MHC I presentation, nanoparticles have to be localized in the cytosol (Kim et al., 2019), potentially indicating a differential localization between rigid and tangled MWCNTs, linked to different internalization methods. TLR2 and TLR4-receptor mediated recognition of MWCNTs has been linked to increased secretion of proinflammatory cytokines (David et al., 2016; Halappanavar et al., 2020; Mukherjee et al., 2018), supporting the dose-dependent secretion of IL1B after 24 h of tangled MWCNT exposure seen in our immunotoxicity assay (Fig. 3). Moreover, TLR can be activated by proinflammatory cytokines (Soares-Silva et al., 2016), suggesting an additive effect from autocrine and paracrine signaling. Taken together, enrichment analysis suggests differential recognition, internalization and localization of tangled versus rigid MWCNTs, explains the differences in their immunotoxic potentials.

4. Conclusion

Due to the unique properties of nanomaterials, the effectiveness of traditional toxicity assays for their hazard assessment has been brought into question, and there is a growing call for nanomaterial toxicity assays that provide a mechanistic understanding of potential toxic effects onset by exposure (Smith et al., 2014; Dusinska et al., 2017). In this study, we exposed THP-1 macrophages to MWCNTs to scrutinize carbon nanotube immunotoxic potential. We used dose-dependent cytokine secretion, informed by transcriptomics analysis, as an endpoint. Using this approach (Fig. 1), we gained further insight into how the critical intrinsic properties of MWCNTs, such as structure, length and aspect ratio, can affect cytotoxicity, immunotoxicity and inflammatory profile. Through a cytotoxicity assay, which was used in dose-selection for immunotoxicity assay, we showed that short and rigid MWCNTs were the most cytotoxic. Selecting equipotent sublethal doses (IC5, IC10 and IC20) for MWCNT exposures in a cytokine secretion assay, tangled and low aspect ratio MWCNTs caused most immunomodulation through the dose-dependent secretion of IL1B. Going beyond traditional approaches, we explored the MOA of MWCNT immunotoxicity using a novel multi-layer correlation analysis, coupling cytokine secretion measurements with transcriptomics. In doing so, long MWCNTs were shown to have a

higher percentage of genes correlating with proinflammatory cytokine secretion, indicating MWCNT length was not only important in cytotoxicity, but also for mediating inflammatory profiles at sublethal exposure concentrations. This multilayer correlation analysis also revealed tangled materials have greater immunomodulatory potency, based on the number of genes associated with cytokine secretion, corroborating our dose-dependent cytokine secretion finding that tangled MWCNTs also induced greater immunotoxicity than rigid MWCNTs. Finally, enrichment terms for those genes discovered in the multilayer analysis showed the mechanism of MWCNT immunotoxicity is conveyed by immune system, signal transduction and pattern recognition associated pathways, and that tangled MWCNTs are distinctly recognized, internalized, processed and presented by macrophages. With these MWCNTs, we observed a clear difference between the immunotoxicity of tangled and rigid MWCNTs. However, further studies are required with both tangled and rigid MWCNTs with similar lengths and aspect ratios to clarify this trend with a larger scope of MWCNTs.

Author contributions

V.H. executed the experimental work, analyzed the data and drafted the manuscript, J.M. interpreted the data and drafted the manuscript, L.A.S. analyzed the data, J.B. supported experimental work, T.T. advised experimental planning, A.S. supervised the data analysis, D.G. conceived and supervised the project.

CRedit authorship contribution statement

Veera Hautanen: Conceptualization, Data curation, Formal analysis, Investigation, Methodology, Project administration, Visualization, Writing – original draft, Writing – review & editing. **Jack Morikka:** Investigation, Writing – original draft, Writing – review & editing. **Laura Aliisa Saarimäki:** Formal analysis, Investigation. **Jan Bisenberger:** Investigation, Methodology. **Tarja Toimela:** Investigation, Methodology. **Angela Serra:** Formal analysis, Investigation, Methodology. **Dario Greco:** Conceptualization, Funding acquisition, Project administration, Resources, Supervision, Writing – original draft, Writing – review & editing.

Declaration of Competing Interest

The authors declare no competing interests.

Data availability

Data is publicly available

Acknowledgements

This work received funding from the EU Horizon 2020 project NanoinformaTIX (grant agreement no. 814426), the Academy of Finland (grant agreement no. 322761), and the European Research Council (ERC) programme, Consolidator project ARCHIMEDES (grant agreement no. 101043848). A.S. was supported by the Tampere Institute for Advanced Study.

The authors would further like to thank Marika Mannerström for her information on THP-1 cell culture and Pia Kinaret and Altoma Rashed for their recommendations in the planning of the study and Altoma Rashed for providing the NM400 and NM401 MWCNTs.

Appendix A. Supplementary data

Supplementary data to this article can be found online at <https://doi.org/10.1016/j.impact.2023.100476>.

References

- Adler, M., Mayo, A., Zhou, X., Franklin, R.A., Meizlish, M.L., Medzhitov, R., et al., 2020 Feb 21. Principles of cell circuits for tissue repair and fibrosis. *iScience*. 23 (2), 100841.
- Banchereau, J., Pascual, V., O'Garra, A., 2012 Oct. From IL-2 to IL-37: the expanding spectrum of anti-inflammatory cytokines. *Nat. Immunol.* 13 (10), 925–931.
- Beg, S., Rizwan, M., Sheikh, A.M., Hasnain, M.S., Anwer, K., Kohli, K., 2011 Feb. Advancement in carbon nanotubes: basics, biomedical applications and toxicity. *J. Pharm. Pharmacol.* 63 (2), 141–163.
- Bihari, P., Vippola, M., Schultes, S., Praetner, M., Khandoga, A.G., Reichel, C.A., et al., 2008 Nov 6. Optimized dispersion of nanoparticles for biological in vitro and in vivo studies. *Part. Fibre. Toxicol.* 5, 14.
- Bosshart, H., Heinzelmann, M., 2016 Nov. THP-1 cells as a model for human monocytes. *Ann. Transl. Med.* 4 (21), 438.
- Bou Zerdan, M., Moussa, S., Atoui, A., Assi, H.I., 2021 Jul 31. Mechanisms of immunotoxicity: stressors and evaluators. *Int. J. Mol. Sci.* 22 (15).
- Braicu, C., Buse, M., Busuioc, C., Drula, R., Gulei, D., Raduly, L., et al., 2019 Oct 22. A comprehensive review on MAPK: a promising therapeutic target in cancer. *Cancers (Basel)*. 11 (10).
- CDC, 2013 Apr. Current Intelligence Bulletin 65: Occupational Exposure to Carbon Nanotubes and Nanofibers. U.S. Department of Health and Human Services, Public Health Service, Centers for Disease Control and Prevention, National Institute for Occupational Safety and Health.
- Chanput, W., Mes, J.J., Wichers, H.J., 2014 Nov. THP-1 cell line: an in vitro cell model for immune modulation approach. *Int. Immunopharmacol.* 23 (1), 37–45.
- Chen, T., Nie, H., Gao, X., Yang, J., Pu, J., Chen, Z., et al., 2014 Apr 21. Epithelial-mesenchymal transition involved in pulmonary fibrosis induced by multi-walled carbon nanotubes via TGF-beta/Smad signaling pathway. *Toxicol. Lett.* 226 (2), 150–162.
- Cheng, Z., Li, M., Dey, R., Chen, Y., 2021 May 31. Nanomaterials for cancer therapy: current progress and perspectives. *J. Hematol. Oncol.* 14 (1), 85.
- David, C.A., Owen, A., Liptrott, N.J., 2016 Jun. Determining the relationship between nanoparticle characteristics and immunotoxicity: key challenges and approaches. *Nanomedicine (London)* 11 (11), 1447–1464.
- De Volder, M.F.L., Tawfick, S.H., Baughman, R.H., Hart, A.J., 2013 Feb 1. Carbon nanotubes: present and future commercial applications. *Science*. 339 (6119), 535–539.
- Dieter, R.R., Holsapple, M.P., 2007 Jan. Methodologies for developmental immunotoxicity (DIT) testing. *Methods*. 41 (1), 123–131.
- Donaldson, K., Murphy, F.A., Duffin, R., Poland, C.A., 2010 Mar 22. Asbestos, carbon nanotubes and the pleural mesothelium: a review of the hypothesis regarding the role of long fibre retention in the parietal pleura, inflammation and mesothelioma. *Part. Fibre. Toxicol.* 7, 5.
- Dong, J., Ma, Q., 2018 Mar. Macrophage polarization and activation at the interface of multi-walled carbon nanotube-induced pulmonary inflammation and fibrosis. *Nanotoxicology*. 12 (2), 153–168.
- Dong, J., Ma, Q., 2018 May 22. Type 2 immune mechanisms in carbon nanotube-induced lung fibrosis. *Front. Immunol.* 9, 1120.
- Dong, X., Liu, L., Zhu, D., Zhang, H., Leng, X., 2015 Jun 3. Transactivator of transcription (TAT) peptide-chitosan functionalized multiwalled carbon nanotubes as a potential drug delivery vehicle for cancer therapy. *Int. J. Nanomedicine* 10, 3829–3840.
- Dong, J., Porter, D.W., Batteli, L.A., Wolfarth, M.G., Richardson, D.L., Ma, Q., 2015 Apr. Pathologic and molecular profiling of rapid-onset fibrosis and inflammation induced by multi-walled carbon nanotubes. *Arch. Toxicol.* 89 (4), 621–633.
- Dusinska, M., Tulinska, J., El Yamani, N., Kuricova, M., Liskova, A., Rollerova, E., et al., 2017 Nov. Immunotoxicity, genotoxicity and epigenetic toxicity of nanomaterials: new strategies for toxicity testing? *Food Chem. Toxicol.* 109 (Pt 1), 797–811.
- Elsabahi, M., Wooley, K.L., 2013 Jun 21. Cytokines as biomarkers of nanoparticle immunotoxicity. *Chem. Soc. Rev.* 42 (12), 5552–5576.
- Fiers, W., Beyaert, R., Declercq, W., Vandenaebale, P., 1999 Dec 16. More than one way to die: apoptosis, necrosis and reactive oxygen damage. *Oncogene*. 18 (54), 7719–7730.
- Foroozandeh, P., Aziz, A.A., 2018 Dec. Insight into cellular uptake and intracellular trafficking of nanoparticles. *Nanoscale Res. Lett.* 13 (1), 339.
- Fraser, K., Kodali, V., Yanamala, N., Birch, M.E., Cena, L., Casuccio, G., et al., 2020 Dec 7. Physicochemical characterization and genotoxicity of the broad class of carbon nanotubes and nanofibers used or produced in U.S. facilities. *Part. Fibre. Toxicol.* 17 (1), 62.
- Fukushima, S., Kasai, T., Umeda, Y., Ohnishi, M., Sasaki, T., Matsumoto, M., 2018 Jan 25. Carcinogenicity of multi-walled carbon nanotubes: challenging issue on hazard assessment. *J. Occup. Health* 60 (1), 10–30.
- Gangwal, S., Brown, J.S., Wang, A., Houck, K.A., Dix, D.J., Kavlock, R.J., et al., 2011 Nov. Informing selection of nanomaterial concentrations for ToxCast in vitro testing based on occupational exposure potential. *Environ. Health Perspect.* 119 (11), 1539–1546.
- Gao, C., Weisman, D., Lan, J., Gou, N., Gu, A.Z., 2015 Apr 7. Toxicity mechanisms identification via gene set enrichment analysis of time-series toxicogenomics data: impact of time and concentration. *Environ. Sci. Technol.* 49 (7), 4618–4626.
- Gou, N., Onnis-Hayden, A., Gu, A.Z., 2010 Aug 1. Mechanistic toxicity assessment of nanomaterials by whole-cell-array stress genes expression analysis. *Environ. Sci. Technol.* 44 (15), 5964–5970.
- Halappanavar, S., van den Brule, S., Nymark, P., Gaté, L., Seidel, C., Valentino, S., et al., 2020 May 25. Adverse outcome pathways as a tool for the design of testing strategies to support the safety assessment of emerging advanced materials at the nanoscale. *Part. Fibre. Toxicol.* 17 (1), 16.

- Hamilton, R.F., Wu, Z., Mitra, S., Shaw, P.K., Holian, A., 2013 Nov 13. Effect of MWCNT size, carboxylation, and purification on in vitro and in vivo toxicity, inflammation and lung pathology. *Part. Fibre. Toxicol.* 10 (1), 57.
- Hockley, S.L., Arlt, V.M., Brewer, D., Giddings, L., Phillips, D.H., 2006 Oct 16. Time- and concentration-dependent changes in gene expression induced by benzo(a)pyrene in two human cell lines, MCF-7 and HepG2. *BMC Genomics* 7, 260.
- Horstmann, C., Davenport, V., Zhang, M., Peters, A., Kim, K., 2021 May 23. Transcriptome profile alterations with carbon nanotubes, quantum dots, and silver nanoparticles: a review. *Genes (Basel)* 12 (6).
- Joris, F., Manshian, B.B., Peynshaert, K., De Smedt, S.C., Braeckmans, K., Soenen, S.J., 2013 Nov 7. Assessing nanoparticle toxicity in cell-based assays: influence of cell culture parameters and optimized models for bridging the in vitro-in vivo gap. *Chem. Soc. Rev.* 42 (21), 8339–8359.
- Joseph, P., 2017 Nov. Transcriptomics in toxicology. *Food Chem. Toxicol.* 109 (Pt 1), 650–662.
- Kim, C.G., Kye, Y.-C., Yun, C.-H., 2019 Nov 15. The role of nanovaccine in cross-presentation of antigen-presenting cells for the activation of CD8+ T cell responses. *Pharmaceutics*. 11 (11).
- Kinaret, P., Ilves, M., Fortino, V., Rydman, E., Karisola, P., Lähde, A., et al., 2017 Jan 24. Inhalation and oropharyngeal aspiration exposure to rod-like carbon nanotubes induce similar airway inflammation and biological responses in mouse lungs. *ACS Nano* 11 (1), 291–303.
- Kinaret, P.A.S., Scala, G., Federico, A., Sund, J., Greco, D., 2020 May. Carbon nanomaterials promote M1/M2 macrophage activation. *Small*. 16 (21), e1907609.
- Klumpp, C., Kostarellos, K., Prato, M., Bianco, A., 2006 Mar. Functionalized carbon nanotubes as emerging nanovectors for the delivery of therapeutics. *Biochim. Biophys. Acta* 1758 (3), 404–412.
- Kobayashi, N., Izumi, H., Morimoto, Y., 2017 Sep 28. Review of toxicity studies of carbon nanotubes. *J. Occup. Health* 59 (5), 394–407.
- Lacy, P., 2006 Sep 15. Mechanisms of degranulation in neutrophils. *Allergy, Asthma Clin. Immunol.* 2 (3), 98–108.
- Leek, J.T., Johnson, W.E., Parker, H.S., Jaffe, A.E., Storey, J.D., 2012 Mar 15. The sva package for removing batch effects and other unwanted variation in high-throughput experiments. *Bioinformatics*. 28 (6), 882–883.
- Liu, Y., Hardie, J., Zhang, X., Rotello, V.M., 2017 Dec. Effects of engineered nanoparticles on the innate immune system. *Semin. Immunol.* 34, 25–32.
- Loret, T., de Luna, L.A.V., Fordham, A., Arshad, A., Barr, K., Lozano, N., et al., 2022 Apr. Innate but not adaptive immunity regulates lung recovery from chronic exposure to graphene oxide nanosheets. *Adv. Sci. (Weinh)*. 9 (11), e2104559.
- Manzanares, D., Ceña, V., 2020 Apr 17. Endocytosis: the nanoparticle and submicron nanocomposites gateway into the cell. *Pharmaceutics*. 12 (4).
- Marwah, V.S., Scala, G., Kinaret, P.A.S., Serra, A., Alenius, H., Fortino, V., et al., 2019 Jan 29. eUTOPIA: solUTion for omics data Preprocessing and analysis. *Source Code Biol. Med.* 14, 1.
- Meng, J., Li, X., Wang, C., Guo, H., Liu, J., Xu, H., 2015 Feb 11. Carbon nanotubes activate macrophages into a M1/M2 mixed status: recruiting naive macrophages and supporting angiogenesis. *ACS Appl. Mater. Interfaces* 7 (5), 3180–3188.
- Mercer, R.R., Scabilloni, J.F., Hubbs, A.F., Battelli, L.A., McKinney, W., Friend, S., et al., 2013 Jul 30. Distribution and fibrotic response following inhalation exposure to multi-walled carbon nanotubes. *Part. Fibre. Toxicol.* 10, 33.
- Misharin, A.V., Morales-Nebreda, L., Reyfman, P.A., Cuda, C.M., Walter, J.M., McQuattie-Pimentel, A.C., et al., 2017 Aug 7. Monocyte-derived alveolar macrophages drive lung fibrosis and persist in the lung over the life span. *J. Exp. Med.* 214 (8), 2387–2404.
- Moore, B.B., Paine, R., Christensen, P.J., Moore, T.A., Sitterding, S., Ngan, R., et al., 2001 Oct 15. Protection from pulmonary fibrosis in the absence of CCR2 signaling. *J. Immunol.* 167 (8), 4368–4377.
- Mukherjee, S.P., Bondarenko, O., Kohonen, P., Andón, F.T., Bzricová, T., Gessner, I., et al., 2018 Jan 18. Macrophage sensing of single-walled carbon nanotubes via toll-like receptors. *Sci. Rep.* 8 (1), 1115.
- Murphy, F.A., Schinwald, A., Poland, C.A., Donaldson, K., 2012 Apr 3. The mechanism of pleural inflammation by long carbon nanotubes: interaction of long fibres with macrophages stimulates them to amplify pro-inflammatory responses in mesothelial cells. *Part. Fibre. Toxicol.* 9, 8.
- Murray, R.Z., Stow, J.L., 2014 Oct 27. Cytokine secretion in macrophages: snares, rabs, and membrane trafficking. *Front. Immunol.* 5, 538.
- Nagai, H., Okazaki, Y., Chew, S.H., Misawa, N., Yamashita, Y., Akatsuka, S., et al., 2011 Dec 6. Diameter and rigidity of multiwalled carbon nanotubes are critical factors in mesothelial injury and carcinogenesis. *Proc. Natl. Acad. Sci. U. S. A.* 108 (49), E1330–E1338.
- Oberdörster, G., Castranova, V., Asgharian, B., Sayre, P., 2015. Inhalation exposure to carbon nanotubes (CNT) and carbon nanofibers (CNF): methodology and dosimetry. *J. Toxicol. Environ. Health B Crit. Rev.* 18 (3–4), 121–212.
- Ogawa, T., Shichino, S., Ueha, S., Matsushima, K., 2021 Nov 25. Macrophages in lung fibrosis. *Int. Immunol.* 33 (12), 665–671.
- Ott, L.W., Resing, K.A., Sizemore, A.W., Heyen, J.W., Cocklin, R.R., Pedrick, N.M., et al., 2007 Jun. Tumor necrosis factor-alpha- and interleukin-1-induced cellular responses: coupling proteomic and genomic information. *J. Proteome Res.* 6 (6), 2176–2185.
- Poulsen, S.S., Jackson, P., Kling, K., Knudsen, K.B., Skaug, V., Kyjovska, Z.O., et al., 2016 Nov. Multi-walled carbon nanotube physicochemical properties predict pulmonary inflammation and genotoxicity. *Nanotoxicology*. 10 (9), 1263–1275.
- Prame Kumar, K., Nicholls, A.J., Wong, C.H.Y., 2018 Mar. Partners in crime: neutrophils and monocytes/macrophages in inflammation and disease. *Cell Tissue Res.* 371 (3), 551–565.
- Rasmussen, K., Mast, J., De Temmerman, P.-J., Verleysen, E., Waegeneers, N., 2014. Multi-Walled Carbon Nanotubes, NM-400, NM-401, NM-402, NM-403, Characterisation and Physico-Chemical Properties. Publications Office of the EU.
- Ritchie, M.E., Phipson, B., Wu, D., Hu, Y., Law, C.W., Shi, W., et al., 2015 Apr 20. Limma powers differential expression analyses for RNA-sequencing and microarray studies. *Nucleic Acids Res.* 43 (7), e47.
- Rydman, E.M., Ilves, M., Koivisto, A.J., Kinaret, P.A.S., Fortino, V., Savinko, T.S., et al., 2014 Oct 16. Inhalation of rod-like carbon nanotubes causes unconventional allergic airway inflammation. *Part. Fibre. Toxicol.* 11, 48.
- Sargent, L.M., Porter, D.W., Staska, L.M., Hubbs, A.F., Lowry, D.T., Battelli, L., et al., 2014 Jan 9. Promotion of lung adenocarcinoma following inhalation exposure to multi-walled carbon nanotubes. *Part. Fibre. Toxicol.* 11, 3.
- Scala, G., Kinaret, P., Marwah, V., Sund, J., Fortino, V., Greco, D., 2018 Jul. Multi-omics analysis of ten carbon nanomaterials effects highlights cell type specific patterns of molecular regulation and adaptation. *Nanotoxicology*. 11, 99–108.
- Scala, G., Serra, A., Marwah, V.S., Saarimäki, L.A., Greco, D., 2019 Feb 15. FunMappOne: a tool to hierarchically organize and visually navigate functional gene annotations in multiple experiments. *BMC Bioinform.* 20 (1), 79.
- Scala, G., Delaval, M.N., Mukherjee, S.P., Federico, A., Khaliullin TO, Yanamala, N., et al., 2021 Jun. Multi-walled carbon nanotubes elicit concordant changes in DNA methylation and gene expression following long-term pulmonary exposure in mice. *Carbon N Y.* 178, 563–572.
- Septiadi, D., Rodriguez-Lorenzo, L., Balog, S., Spuch-Calvar, M., Spiaggia, G., Taladriz-Blanco, P., et al., 2019 Dec 11. Quantification of carbon nanotube doses in adherent cell culture assays using UV-VIS-NIR spectroscopy. *Nanomaterials (Basel)*. 9 (12).
- Serra, A., Saarimäki, L.A., Fratello, M., Marwah, V.S., Greco, D., 2020 May 1. BMDx: a graphical shiny application to perform benchmark dose analysis for transcriptomics data. *Bioinformatics*. 36 (9), 2932–2933.
- Sharma, M., Nikota, J., Halappanavar, S., Castranova, V., Rothen-Rutishauser, B., Clippinger, A.J., 2016 Jul. Predicting pulmonary fibrosis in humans after exposure to multi-walled carbon nanotubes (MWCNTs). *Arch. Toxicol.* 90 (7), 1605–1622.
- Smith, M.J., Brown, J.M., Zamboni, W.C., Walker, N.J., 2014 Apr. From immunotoxicity to nanotherapy: the effects of nanomaterials on the immune system. *Toxicol. Sci.* 138 (2), 249–255.
- Soares-Silva, M., Diniz, F.F., Gomes, G.N., Bahia, D., 2016 Feb 24. The mitogen-activated protein kinase (MAPK) pathway: role in immune evasion by trypanosomatids. *Front. Microbiol.* (7), 183.
- Sohaebuddin, S.K., Thevenot, P.T., Baker, D., Eaton, J.W., Tang, L., 2010 Aug 21. Nanomaterial cytotoxicity is composition, size, and cell type dependent. *Part. Fibre. Toxicol.* 7, 22.
- Stella, G.M., D'Agnano, V., Piloni, D., Saracino, L., Lettieri, S., Mariani, F., et al., 2022 Mar. The oncogenic landscape of the idiopathic pulmonary fibrosis: a narrative review. *Transl. Lung Cancer Res.* 11 (3), 472–496.
- Tsuchiya, S., Yamabe, M., Yamaguchi, Y., Kobayashi, Y., Konno, T., Tada, K., 1980 Aug. Establishment and characterization of a human acute monocytic leukemia cell line (THP-1). *Int. J. Cancer* 26 (2), 171–176.
- Umeda, Y., Kasai, T., Saito, M., Kondo, H., Toyota, T., Aiso, S., et al., 2013 Jun. Two-week toxicity of multi-walled carbon nanotubes by whole-body inhalation exposure in rats. *J. Toxicol. Pathol.* 26 (2), 131–140.
- Vippola, M., Bard, D., Sarlin, E., Tuomi, T., Tossavainen, A., 2009. NanoAtlas of Selected Engineered Nanoparticles. Finnish Institute of Occupational Health.
- Wendisch, D., Dietrich, O., Mari, T., von Stillfried, S., Ibarra, I.L., Mittermaier, M., et al., 2021 Dec 22. SARS-CoV-2 infection triggers profibrotic macrophage responses and lung fibrosis. *Cell*. 184 (26), 6243–6261.e27.
- Wynn, T.A., 2008 Jan. Cellular and molecular mechanisms of fibrosis. *J. Pathol.* 214 (2), 199–210.
- Yang, L., Allen, B.C., Thomas, R.S., 2007 Oct 25. BMDExpress: a software tool for the benchmark dose analyses of genomic data. *BMC Genomics* (8), 387.
- Yang, L., Zhou, F., Zheng, D., Wang, D., Li, X., Zhao, C., et al., 2021 Dec. FGF/FGFR signaling: from lung development to respiratory diseases. *Cytokine Growth Factor Rev.* 62, 94–104.
- Zhang, J.-M., An, J., 2007. Cytokines, inflammation, and pain. *Int. Anesthesiol. Clin.* 45 (2), 27–37.